Available online at www.sciencedirect.com
ScienceDirect
European Journal of Pharmaceutics and Biopharmaceutics 67 (2007) 621–631
European Journal of Pharmaceutics and Biopharmaceutics
www.elsevier.com/locate/ejpb

Research paper

Nanoparticles based on the complex of chitosan and polyaspartic acid sodium salt: Preparation, characterization and the use for 5-fluorouracil delivery

Yongli Zheng [a], Wuli Yang [a,*], Changchun Wang [a], Jianhua Hu [a], Shoukuan Fu [a], Ling Dong [b], Lili Wu [b], Xizhong Shen [b]

[a] *Department of Macromolecular Science, Fudan University, Shanghai, China*
[b] *Zhongshan Hospital, Fudan University, Shanghai, China*

Received 9 September 2006; accepted in revised form 5 April 2007
Available online 19 April 2007

Abstract

New nonstoichiometric polyelectrolyte complex nanoparticles were prepared based on chitosan (CS) and polyaspartic acid sodium salt (PAsp). The physicochemical properties of the complexes were investigated by means of turbidity, dynamic light scattering, transmission electron microscopy and zeta potential. The results indicated that the slow dropwise addition of chitosan into PAsp allowed to elaborate either anionic or cationic particles in the size range of 85–300 nm with proper CS and PAsp unit molar ratios. Investigation of structural changes during the addition of CS revealed that the microstructure of the nanoparticles depended strongly on the unit molar ratio of CS to PAsp. Nanoparticles containing a hydrophilic drug, 5-fluorouracil (5FU), were prepared by mixing and absorption method. In vitro and in vivo experiment indicated that the drug-loaded CS-PAsp nanoparticles presented a sustained release of 5FU compared to the 5FU solution and the areas under curve (AUC) were increased by about four times.

Keywords: Chitosan; Polyaspartic acid; Nanoparticle; Controlled drug release; 5-Fluorouracil

1. Introduction

Nanoparticles made of polyelectrolytes complexation (PEC) have shown potential for use as drug delivery systems [1,2]. Polyelectrolyte complexes are formed by interactions between macromolecules that carry oppositely charged ionisable groups [3]. During the last years PECs on the base of natural and synthetic polymers evoke a particular interest. Chitosan, whose structure is shown in Fig. 1a, is a well-known natural cationic polyelectrolyte that processes primary amine groups ($-NH_2$) and can be protonated in acidic environments to become $-NH_3^+$. It is a partially deacetylated form of chitin, which is a structural polysaccharide found in crustacea, insects, and some fungi, and it has attracted interest as a biocompatible, stimulus–responsive, mucoadhesive material for use in biomedical applications [4–6]. Recently the use of complexation of oppositely charged macromolecules to prepare CS complexes and nanoparticulate structures as controlled drug-release formulations has attracted much attention [7–11], because this process is simple, feasible, and can usually be performed under mild conditions.

Polyaspartic acid (Fig. 1b) or its salts is a kind of newly biodegradable, innocuous and environmental friendly bioorganic polymer, recognized as green material, and widely applied in such areas as agriculture, medicine, commodity, water treatment petroleum, etc. [12–15]. Recently the synthesis and application of polyaspartic acid has been studied

* Corresponding author. Key Laboratory of Molecular Engineering of Polymers of Educational Ministry, Department of Macromolecular Science, Fudan University, Shanghai 200433, China. Tel.: +86 21 65642385; fax: +86 21 65640293.
E-mail address: wlyang@fudan.edu.cn (W. Yang).

0939-6411/$ - see front matter © 2007 Elsevier B.V. All rights reserved.
doi:10.1016/j.ejpb.2007.04.007

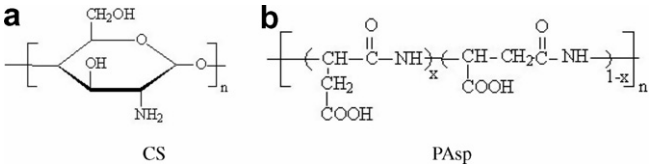

Fig. 1. Chemical structures of CS and PAsp.

in many companies. However, little work was focused on the complex of chitosan and polyaspartic acid.

For more than four decades the antineoplastic agent, 5-fluorouracil (5FU), has been widely used in the therapy of different solid tumor types such as cancer of the stomach, liver, intestine, and so on. Because of the short plasma half-life of 10–20 min, high doses, e.g. 400–600 mg/m^2, have to be administered weekly, to reach a therapeutic drug level [16]. However, 5FU may cause the following adverse effects: bone marrow depression, gastrointestinal tract reaction, or even leucopenia and thrombocytopenia [17]. It has been recognized that, optimally, this drug should be dosed once or twice a week, preferably a long-acting injectable and targeted to the desired sites [18]. Polymer systems can be used to physically trap an antitumor agent and release it in a sustained form directly at the tumor site [19,20]. Among the drug delivery strategies intended to supply sustained release, the use of CS complexes has shown a significant degree of success. More concretely, in our laboratory, we have developed nanocarriers made of CS which have shown a great capacity in drug controlled release [10,21]. In this context, the use of CS-PAsp nanoparticles could be a useful approach to concentrate the loaded drug on the focus of the disease. This would result in an increase in the therapeutic index of the loaded molecule by reducing both the given and the side effects. The purpose of present study was to obtain stable complexes of nanoparticles from CS and polyaspartic acid sodium salt (PAsp) which could embed 5FU with a relatively load capacity. The effect of preparation condition and external parameters on the morphology of the nanoparticles was studied in detail. Furthermore, the preliminary release properties of the drug-loaded nanoparticles of CS–PAsp have been studied in vitro and vivo.

2. Materials and methods

2.1. Materials

Chitosan (CS, the degree of deacetylation (DD) was 95.3%) was purchased from Shanghai Kabo Trading Co., Ltd. (Shanghai, China), and the weight average molecular weights (Mws) of CS were about 17.9 kDa. The Mws were determined by viscometric methods [22]. Polyaspartic acid sodium salt (PAsp) was prepared in our laboratory according to the reference [23]. The weight average molecular weights (Mws) of PAsp were 5.0 kDa. 5-fluorouracil (5FU, 99%) was purchased from Shanghai Xudong Haipu Pharmaceutical Co., Ltd. (Shanghai, China). All other chemicals were of analytical grade and used without further purification.

2.2. Preparation of CS–PAsp nanoparticles

CS–PAsp nanoparticles were prepared by mixing a positively charged CS acetic acid solution and a negatively charged PAsp solution at room temperature. Briefly, 1.0 g of CS was dissolved in dilute acetic acid solution (1.0 g CH_3COOH + 100 g deionized water) and the solution was stirred for 24 h, and then filtered by paper filter for use. 1.0 g PAsp was dissolved in 100 g deionized water, stirred for 6 h and then filtered by paper filter for use. Afterwards, the PAsp solution was used as a base material and the CS solution was dropped into it in different ratio at a dropping rate of one drop per second with a syringe under magnetic stirring. The opalescent suspension was formed. The obtained suspension was then filtered by paper filter for characterization.

Drug-loaded CS-PAsp nanoparticles were prepared by two methods. Firstly, the mixture solution of 5FU and CS was dropped into the PAsp solution. The process was the same as discussed in preparation of CS-PAsp nanoparticles (mixing method, CS-PAsp-m). Secondly, the 5FU solution was added into the suspension of CS-PAsp nanoparticles. This mixture was magnetically stirred for two hours under room temperature (absorption method, CS-PAsp-a).

Glutaraldehyde (GLA) cross-linking nanoparticles were prepared as follows: a known mass of 0.25% (w/w) GLA solution was dropped in CS–PAsp suspension or drug-loaded CS–PAsp suspension under magnetic stirring. This mixture was further stirred for three hours under room temperature (G-CS–PAsp, G-CS–PAsp-m and G-CS–PAsp-a).

2.3. Determination of encapsulation efficiency and loading capacity

To determine the encapsulation efficiency (EE) and loading capacity (LC), CS-PAsp encapsulating 5FU nanoparticles were separated from the aqueous suspension medium by ultra centrifugation with 145,000*g* at 25 °C for 30 min. Washed by dilute acetic acid (pH 5.0) solution and separated by ultracentrifugation three times, the precipitate was frozen by liquid nitrogen and lyophilized by freeze dryer system to obtain dried CS-PAsp nanoparticles. A known mass of dried nanoparticles was dissolved in dilute hydrochloric acid solution (pH 1.0) and the amount of 5FU in this solution was measured by HPLC. HPLC was carried out using a LC-4A HPLC system equipped with a LC-4A pump, and a SPD-10A UV detector (Shimadzu, Kyoto, Japan). The detective wavelength was set at 270 nm. HPLC analysis of samples was performed using a Science C18 column (4.6 × 250 mm, 5 μm, Japan) preceded by a C18 guard column (GL Sciences, Japan). The column temperature was maintained at room temperature. The mobile phase was a mixture of methanol/3.6% acetic acid (80:20, v/v). The flow rate was main-

tained at 1.0 mL/min. Each sample was repeatedly measured 3 times and the values reported were mean values for two replicate samples. The 5FU concentration range used to construct calibration curve was from 0.005 to 0.1 mg/mL. The 5FU encapsulation efficiency of the process and the 5FU loading capacity of the nanoparticles were calculated with the following equation:

$$\mathrm{EE} = \frac{\text{The amount of 5FU in the nanoparticles}}{\text{Total amount of 5FU}} \times 100\%$$

$$\mathrm{LC} = \frac{\text{The amount of 5FU in the nanoparticles}}{\text{Total amount of nanoparticles weight}} \times 100\%$$

2.4. In vitro drug release from the nanoparticles

Dried CS-PAsp encapsulating 5FU nanoparticles were prepared as described in experiment section (determination of encapsulation efficiency and loading capacity), then redispersed in 4.0 mL of phosphate-buffered saline (PBS) (pH 7.4, $I = 0.3$) and placed in a dialysis membrane bag with a molecular weight cut-off of 5.0 kDa, tied and placed into 40.0 mL of PBS medium. The entire system was kept at 37 ± 0.5 °C in a beaker (220 ± 2 r/min). After a predetermined period, 3.0 mL of the medium was removed and the amount of 5FU was analyzed by HPLC measurement. The released 5FU was determined by a calibration curve. In order to maintain the original volume, each time, 3.0 mL fresh PBS solution was added to the system. The 5FU release experiments were repeated three times. Bringing into comparison, the release of 5FU from the dialysis bag under the same conditions was also evaluated.

2.5. In vivo drug release from the nanoparticles

Female kunming mice (Certificate: SCXK (Shanghai) 2002-0002) weighing between 20 and 25 g were used. These mice were randomly divided into three groups with sixty mice in each group, one group for administration with 5-fluorouracil solution (1.25 mg/mL) at a dose of 30 mg/kg and other groups for drug-loaded nanoparticles at an equivalent drug dose to the 5FU group. At 15 min after administration, about 1 mL of blood sample was drawn from the neck veil of a mouse. Blood samples at this time point were drawn repeatedly from six mice. Every six mice were used to prepared blood sample with the same procedure at 1, 2, 4, 6, 8, 12, 16, 24 and 48 h, respectively. All blood samples were collected in heparinized tubes and were immediately centrifuged. Plasma samples were obtained and stored in a −20 °C freezer until analysis. 5FU concentrations in mice plasma samples were measured using HPLC method. Average extraction recovery was greater than 90% for the method.

2.6. Characterization and measurement

The turbidity of the complex dispersions was measured at $\lambda = 500$ nm with a Perkin-Elmer Lambda 35 UV–vis spectrophotometer. The device indicated the value of transmitted light (transmittance, T), system's turbidity expressed in arbitrary units as $T\%$. At wavelength 500 nm, the polyelectrolytes do not absorb. Deionized water was used to establish the baseline. T was expressed as the average of at least three measurements.

The pH value was measured at 25 ± 1 °C in a PHS-3TC digital pH-meter with an error of 0.01 pH unit. A combined glass electrode E-201 was employed and the pH-meter was calibrated with two buffer solutions supplied by Shanghai Hongbei Reagent Factory.

Hydrodynamic diameter (D_h) and polydispersity index (PI, $\mu_2/\langle\Gamma\rangle^2$) [24] of the CS-PAsp nanoparticles were measured by dynamic light scattering (DLS) in buffer solution with different pH values. A commercial laser light scattering spectrometer (Malvern Autosizer4700) equipped with a multi-τ digital time correlation (Malvern PCS7132) and Compass 315M-100 Diode-Pumped Laser (output power $\geqslant 100$ mW, CW at $\lambda_0 = 532$ nm) as a light source was used. All DLS measurements were done at 25 ± 0.1 °C and at a scattering angle of 90°. The measured time correlation functions were analyzed by automatic progress equipped with the correlator.

The zeta potential of the CS-PAsp nanoparticles was measured at 25 °C with a Zeta Plus zeta potential Analyzer (Brookhaven, USA). The samples were diluted with 0.1 mM NaCl solution at pH 4.5 in order to maintain a constant ionic strength and measured in automatic mode. Each sample was repeatedly measured three times and the values reported were mean values for two replicate samples.

The morphology of the CS-PAsp nanoparticles was obtained using a Hitachi HU-11B transmission electron microscope (TEM) operating at 250 kV. The sample was prepared as follows: A drop of CS-PAsp nanoparticles opalescent suspension was mounted onto carbon-coated copper grid. They were dried at room temperature, and then were examined using a TEM without being negative stained.

3. Results and discussion

3.1. Preparation of CS-PAsp nanoparticles

3.1.1. Formation of particles

The formation of colloidal polyelectrolyte complexes between CS and PAsp was studied as a function of the mixing unit ratio n^+/n^-, i.e., the molar ratio between cationic and anionic units. Four kinds of phenomena were observed in turn during the addition of CS solution into PAsp solution: polyelectrolyte solution, opalescent suspension, flocculation and opalescent suspension. Fig. 2a displays the common feature of the complex process. The transmittance at $\lambda = 500$ nm decreased sharply when n^+/n^- was up to the value described as point 1 ($n^+/n^- = 0.72$) and arrived at the least value at point 2 ($n^+/n^- = 0.88$). Further increase in n^+/n^- led to system flocculation until point 3 ($n^+/$

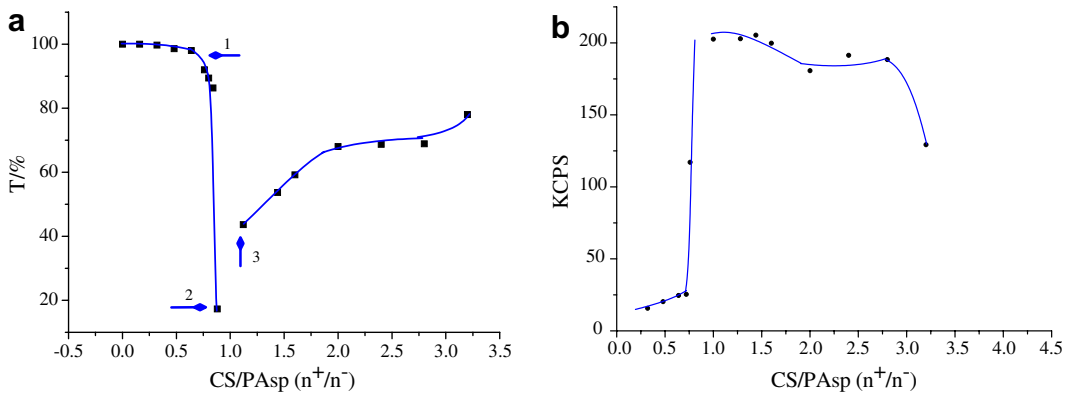

Fig. 2. Transmittance (a) and scattering intensity (b) of CS-PAsp nanoparticles obtained by slow addition of a CS solution to a PAsp solution. Point 1, at which the transmittance at $\lambda = 500$ nm begins to decrease sharply; point 2, at which the transmittance arrives at the least value; point 3, at which the system was opalescent and the transmittance began to increase again.

$n^- = 1.28$), at which system was opalescent and the transmittance began to increase again. This evidenced the formation of insoluble polyelectrolyte complexes since neither CS nor PAsp absorbed light at $\lambda = 500$ nm. The formation of PEC was also confirmed by the increase of the scattering intensity (Fig. 2b). Except for the flocculation of the system characterized by a drop of the optical density, the colloidal dispersions were stable, indicating that electrostatic stabilization prevented further coagulation. This stabilization might be ensured by an excess of binding of the major component, likely to form a stabilizing shell around the particles.

3.1.2. Effect of the molar ratio of CS to PAsp

The particle size and size distribution of CS-PAsp nanoparticles, prepared by dropwise addition of CS into PAsp solution at varying concentration ratio of CS and PAsp, were determined by DLS and the results were displayed in Table 1. As seen in Table 1, there were two particles forming stages (PFS) interrupted by a flocculation stage during the titration. Complex nanoparticles began to form at n^+/n^- 0.72. Increase of n^+/n^- value resulted in the increase of the particles size until n^+/n^- 0.88, at this point flocculation began to form. When the n^+/n^- value was up to 1.28, new kinds of nanoparticles were formed. These results were according to that described in paragraph 3.1.1. For the convenience of discussion, the critical n^+/n^- values at which the particles and flocculation began to form were defined as C_1, C_2, and C_f which were 0.72, 1.28 and 0.88, respectively. The characteristic of the first PFS was the increase of hydrodynamic diameters until the n^+/n^- value was increased up to C_f.

These results indicated that the particle forming stages relied on the formation of hydrophobic segments on polymer chain by charge neutralization and arrangement of these segments into particles stabilized by free unpaired charges, furthermore, the free unpaired charges were different in the two stages of PFS [25]. In the first PFS, PAsp chains were in excess amount and the complexes formed bearing many unpaired negative charges still available for complexation (Table 2). Being more hydrophilic, uncomplexed segments of PAsp constituted the corona of the particles. Addition of more CS led to the observed size increase by forming new hydrophobic segments collapsing on the particles. As the n^+/n^- was up to a value in some range, the complete ion-pairing of PAsp with CS led to quasi-neutral complexes without enough unpaired negative groups to ensure the stabilization of particles. Hence, formed complexes quickly aggregated. Addition of excess CS to PAsp, more charge neutralizations led to the rearrangements of molar chains to form more compact particles with positive charges. Thus, unpaired CS chains

Table 2
The zeta potential of the CS-PAsp nanopartciles

CS/PAsp	0.76	0.80	1.28	1.6	2.4	3.2
Zeta (mV)	−21.08	−16.90	10.46	30.56	51.40	56.98
±AD	1.28	3.02	2.58	3.19	0.92	2.06

pH 4.5.

Table 1
Effect of CS and PAsp molar ratio on the mean size and size distribution

n^+/n^-	0.68	0.72	0.76	0.80	0.88	1.12	1.28	1.6	2.4	2.8	3.2
D_h (nm)	–	98.6[a]	141.5	194.3	F[b]	F	189.3[c]	184.2	187.0	197.3	147.5
PI	–	0.14	0.11	0.08	–	–	0.13	0.09	0.12	0.13	0.13

a, the critical n^+/n^- value where the nanoparticles formed firstly; b, the critical n^+/n^- value where the flocculation occurred; c, the critical n^+/n^- value where the nanoparticles formed secondly; F, flocculation.

constituted the corona of the particles. The arrange process will be discussed in the following section.

3.1.3. The morphology of the CS-PAsp nanoparticles

To observe the morphology and microstructure of CS-PAsp nanoparticles prepared under different n^+/n^- value, TEM examinations were performed. As shown in Fig. 3a, the complete and solid CS-PAsp nanospheres with clear contrast were observed when the n^+/n^- value was 0.72. However, when the n^+/n^- value was in the range of 0.72–0.88, flocculation occurred and no nanoparticle formed. At n^+/n^-1.28, the nanoparticles showed core-shell separation structure (Fig. 3b). When the n^+/n^- value was above 1.28, the core-shell separation structure began to diminish and the particles turned back to dark solid spheres at n^+/n^- 3.2 (Fig. 3c). The mean size based on TEM image at n^+/n^- 3.2 was smaller than that at n^+/n^- 1.28, this result was consistent with the hydrodynamic diameter (Table 1).

The results allowed us to propose a mechanism of the structure arrangement process described as following. Polyelectrolyte complex formation can be described as two-step reaction, where the first fast step is the formation of the initial contacts, which proceeds during the diffusion time of the components and results in the formation of initial aggregates. The second step consists of structural rearrangements via a polyelectrolyte exchange reaction between the chains present in solution. In the formation of highly aggregated complexes, the exchange reactions are suppressed. Once addition of salt solution or the long-chain component is in high excess, exchange reaction is activated and the short-chain component is redistributed between the aggregates and the free long-chain component in solution [26]. In our system, CS was the long-chain component and PAsp was the short-chain one. As CS solution was a mixture of polymers, it contained shorter chains and longer chains. When the n^+/n^- value was 0.72, highly aggregated particles stabilized by unpaired PAsp chain were formed (Fig. 3a). During the increase of n^+/n^- up to 1.28, CS reacted with the unpaired PAsp chain and formed particles with a CS chain shell showing a core-shell

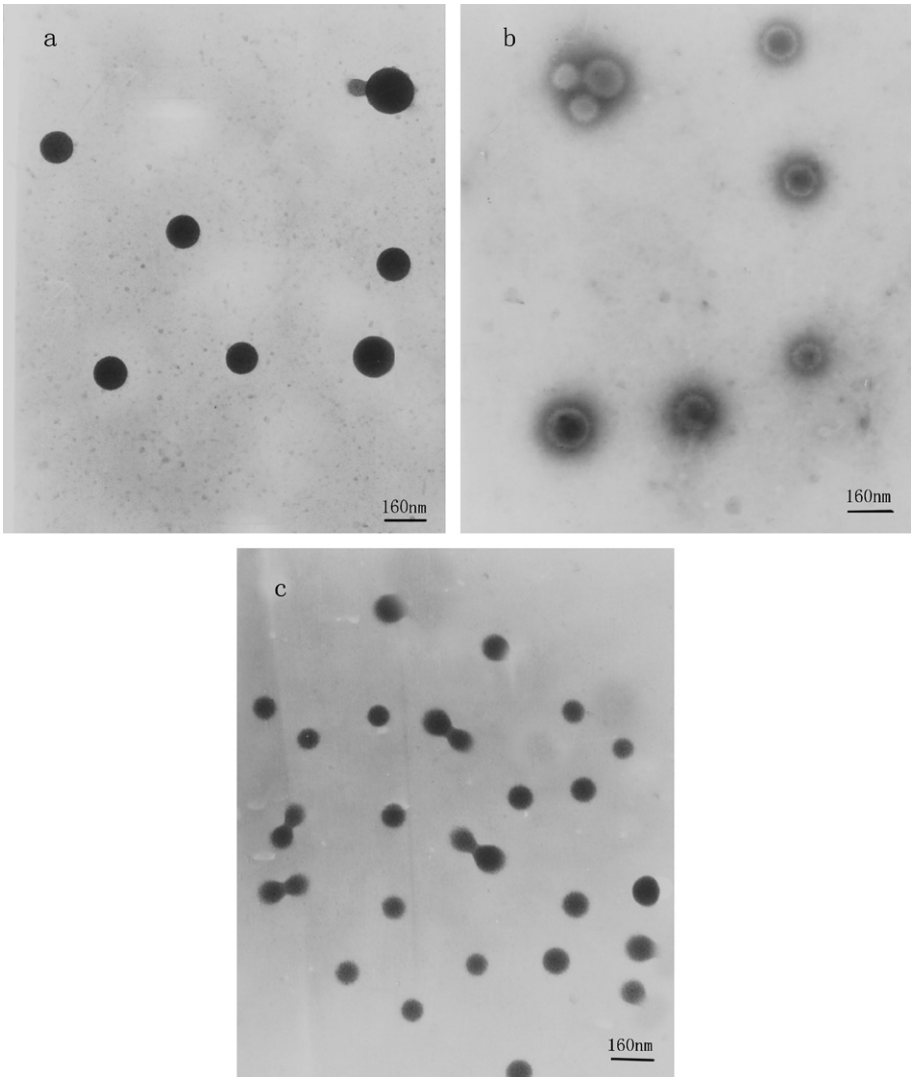

Fig. 3. Morphologies of CS-PAsp nanoparticles at various n^+/n^-. (a) $n^+/n^- = 0.72$; (b) $n^+/n^- = 1.28$; (c) $n^+/n^- = 3.2$.

structure (Fig. 3b) beyond Flocculation [12]. At the point of n^+/n^- 1.28, CS was in a high excess and the exchange reaction was activated. The complexes formed by shorter chain of CS and PAsp were disassociated, and the longer chain CS was preferred to react with the disassociated because of its entropical favor. As n^+/n^- was up to 3.2, the stronger ionic interactions tended to arrange the nanoparticles to a more compass one that showed a smaller size [10] (Fig. 3c).

3.2. Influence of external parameters on the size of the CS-PAsp nanoparticles

3.2.1. Effect of solution pH

CS is a weak base polysaccharide and PAsp is a weak acid salt, therefore, the hydrated size and size distribution of CS-PAsp nanoparticles stabilized by the charged corona of unpaired molecule chain were affected by the pH value of the medium. In this work, CS-PAsp nanoparticles were prepared at a pH of about 4.5, and dilute ammonia or dilute acetic acid was added to obtain different pH values. According to the results in Table 2, CS-PAsp particles were stabilized by two kinds of charged chains. The effect of pH value on the size of the two kinds of particles is shown in Tables 3a and 3b. The size of nanoparticles with n^+/n^- 0.72 did not change significantly at various pH (Table 3a), except the flocculation occurring at pH < 4.15. Increasing n^+/n^- to 3.2 (Table 3b), changing pH in the range of 2.5 to 6.0, the mean size stayed unchangeable, and then a little increase at pH < 2.5. However, when pH was higher than 4.5, the mean size decreased as the increase of pH, then when pH reached 7.0, the mean size increased sharply and aggregation occurred.

These results could be explained as follows: the particles with n^+/n^-0.72 were stabilized by the charged unpaired PAsp chains with a pK_a of 4.5–4.75 [27]. Decreasing pH value to 4.15, the effective over-charge of the particles was reduced to such an extent that precipitation was formed. Due to the small zeta potential of the n^+/n^- 0.72 nanoparticles, the unpaired corona on the surface of the nanoparticles was thin. Thus, the mean size of the particles changed slightly when pH varied in the range of 4.5–7.0. When n^+/n^- was 3.2, the corona of the particles was contributed by charged unpaired CS chain with a pK_a of 6–7 [28]. At pH 2.5, the complexion between CS and PAsp was destroyed partly resulting in more CS chains unpaired, which entwined onto the surface of the nanoparticles leading to the little increase in nanoparticles size. Increasing pH value over 4.5, the protonated glucosamine units were neutralized leading to a collapse of chitosan chains in the particles corona, resulting in the decrease in particles size. Increasing pH to 7.0, increase in particles size suggested that the degree of protonisation at surface of the particles was reduced, decreasing electrostatic repulsion between the particles thereby resulting in the particles aggregation.

3.2.2. Effect of the temperature

To investigate the effect of medium temperature on the particles parameter, the nanoparticles were prepared by adding CS solution to PAsp solution and then incubated for 30 min at different temperature. Table 4 displays the results of the variation in the size and PI of CS–PAsp nanoparticles as function of the incubation temperature. A sharp decrease in particles size was observed for particles at n^+/n^- 0.72 with increasing incubation temperature, conversely to 3.2 ones which changed slightly below 45 °C. The size reduction was probably due to the fact that increasing temperature would decrease the interaction parameter between polyelectrolytes and solvent (water) [29]. Since PAsp chain was softer than CS chain, it had stronger interaction with water. When the cured temperature increased, the mean size of particles at n^+/n^- 0.72 decreased obviously because the PAsp shell layer lost more water. For particles at n^+/n^- 3.2, when the incubation temperature reached 50 °C, the mean size of cationic particles increased because of aggregation of the nanoparticles.

3.2.3. Effect of ionic strength on the stability of the nanoparticles

It is known that the stability of polyionic complexes is strongly influenced by the ionic strength of the medium: being destabilized with an increase in ionic strength due to electrostatic shielding [30]. The influence of salt concentration on the nanoparticles formed from CS and PAsp was therefore determined by measuring the scattering intensity and size of the nanoparticles suspension after the addition of NaCl at various concentrations. The results in Table 5 clearly show, that the nanoparticles size was influenced by the salt concentration. The mean size of anionic particles (n^+/n^- 0.72) increased quickly and irreversible aggregation was observed at once when NaCl solution was added. As NaCl concentration increased, the mean size of cationic particles did not increase until NaCl concentration was up to 1.00 mol/L for n^+/n^- 3.2. For cationic particles (n^+/n^- 3.2), because CS had stiffer backbone and larger molecular weight than PAsp, CS shell may provide some steric stabilization for the particle, then cationic particles could resist higher NaCl concentration. After that, the mean size of the nanoparticles increased quickly and the suspension became clear. This might be because of

Table 3a
Effect of solution pH values on the mean particle size and polydispersity index of the CS-PAsp nanoparticles at $n^+/n^- = 0.72$

pH	4.15	4.5	4.75	5.0	5.25	5.5	6.0	6.5	7.0
D_h	1616.9	195.4	163.3	165.8	164.8	161.6	162.9	163.6	166.9
PI	1.0	0.05	0.08	0.07	0.15	0.18	0.24	0.40	0.40

Table 3b
Effect of solution pH values on the mean particle size and polydispersity index of the CS-PAsp nanoparticles at $n^+/n^- = 3.2$

pH	2.0	2.5	3.0	3.5	4.0	4.5	5.0	5.5	6.0	6.5	7.0
D_h	189.4	165.6	143.9	148.2	145.2	147.3	134.2	118.4	106.6	105.3	598.7
PI	0.1	0.12	0.09	0.12	0.1	0.13	0.09	0.11	0.13	0.11	0.53

Table 4
Influence of incubation temperature on the mean size and PI of the nanoparticles

T (°C)	CS:PAsp			
	0.72		3.2	
	D_h	PI	D_h	PI
25	195.4	0.05	129.3	0.13
30	182.1	0.05	123.5	0.15
35	162.9	0.02	124.2	0.14
40	150.2	0.005	128.5	0.16
45	137.9	0.02	220.0	0.35
50	126.6	0.02	288.0	0.40

Table 5
Influence of NaCl concentration on the mean size and PI of the nanoparticles

NaCl (mol/L)	CS:PAsp (n^+/n^-)			
	0.72		3.2	
	D_h	PI	D_h	PI
0	224.8	0.06	129.3	0.13
0.085	454.1	0.12	130.5	0.13
0.17	714.1	0.13	137.3	0.13
0.34	–	–	134.5	0.12
0.51	–	–	128.6	0.13
0.68	–	–	138.4	0.12
0.85	–	–	149.5	0.16
1.00	–	–	529.6	0.45

the fact that addition of salt resulted in the disassociation of the nanoparticles caused by electrostatic shielding. Hence, it was the electrostatic interaction which was dominant in stabilizing the complex.

3.2.4. Effect of cross-linker concentration

There were a little floccules emerging when the CS-PAsp nanoparticles suspension was placed under room temperature for one month. In order to enhance the stability of the nanoparticles, glutaraldehyde (GLA) was used as a cross-linker added to the suspension. When the unit molar ratio of CS to PAsp was 0.72, a little mount of the GLA solution added to the system resulted in the aggregation of anionic nanoparticles. The mean size of the cross-linked cationic nanoparticles (n^+/n^- 1.44) decreased as GLA concentration increased (Table 6). When GLA cross-linked the amino groups of CS, CS chain would stack tightly, then the mean particle size would decrease. Furthermore, the nanoparticles did not change in the mean size and PI even when being placed under room temperature for 6 months. Thus, it seems safe to conclude that the stability and the mean size of the nanoparticles could be adjusted by adding GLA cross-linker.

Table 6
Effect of GLA concentration on the mean size and PI of cationic G-CS-PAsp nanoparticles

GLA (g)	D_h (nm)	PI
0	184.2	0.09
0.1	175.7	0.08
0.2	146.5	0.09
0.3	141.9	0.08
0.4	140.5	0.10
0.5	Floccule	–

The unit molar ratio of CS to PAsp is 1.44.

3.3. Encapsulation and release of 5FU

5FU, as water-soluble anti-cancer drug, is difficult to be encapsulated by hydrophobic polymer. In this paper, 5FU was loaded into nanoparticles by mixing and absorption method in order to investigate the feasibility of using nanoparticles as hydrophilic drug carriers. The effect of 5FU encapsulation on particles parameter and drug release characterization was investigated systematically.

3.3.1. Loading 5FU by absorption method

In order to investigate the capacity of CS-PAsp nanoparticles to embed 5FU, nanoparticles were immersed into 5FU solution with different concentrations under magnetic stirring for 2 h. Table 7 lists the influence of 5FU on EE and LC of nanoparticles with n^+/n^- 2.8. Although EE decreased with 5FU concentration increase, more 5FU was embedded into nanoparticles leading to a higher LC at 4 mg/mL.

The results in Table 7 show that nanoparticles could embed 5FU. The influence of mixing time on mean size, LC and EE of nanoparticles is shown in Table 8. It could be found that mean size increased drastically once nanoparticles were added into 5FU solution and then increased slowly as stirring time extended. Different from mean size, the increase of EE and LC took place smoothly before the stirring time was up to 2 h. When the stirring time was

Table 7
Encapsulation efficiency (EE) and loading capacity (LC) of CS-PAsp-a nanoparticles loading 5FU by absorption method ($n^+/n^- = 2.8$)

5FU (mg/mL)	1	4	6	10
EE (%)	34.0	30.0	11.0	8.5
LC (%)	10.2	28.6	18.0	22.1

Table 8
Mean size and the drug content of CS-PAsp-a nanoparticles at different absorption time ($n^+/n^- = 2.8$)

Time (h)	D_h	PI	EE (%)	LC (%)
Drug-free	185.8	0.12	0	0
0	242.7	0.19	8.4	10.1
0.5	246.0	0.16	16.8	18.3
1.0	263.3	0.22	24.5	24.6
2.0	283.6	0.31	30.0	28.6
16.0	361.2	0.4	31.2	29.6

EE, encapsulation efficiency; LC, loading capacity.

16 h, EE and LC were not changeable obviously. These results could be explained as follows. When nanoparticles were added into 5FU solution, 5FU was absorbed on the surface of the nanoparticles resulting in a drastic increase in mean size. As stirring time extended, nanoparticles turned from white particles with a dark ring to black solid spheres due to the penetration of 5FU as shown in Fig. 4. After 2 h of stirring, embedment of 5FU in nanoparticles came to a higher level. Further increase of stirring time did not obviously help to enhance EE and LC, because absorption balance might be obtained by about 2 h.

3.3.2. Loading 5FU by mixing method

5FU was also loaded in the nanoparticles by mixing method. Fig. 5 shows that the morphology of nanoparticles loaded 5FU displayed a solid sphere shape whatever n^+/n^-. After drug incorporation, the mean sizes of nanoparticles loading 5FU increased somewhat compared with drug-free nanoparticles, as shown in Table 9. Table 10 shows that encapsulation efficiency (EE) decreased as the increase of the molar ratio of CS and PAsp, correspondingly, loading capacity (LC) increased firstly and then decreased reaching the maximum at the molar ratio of 1.44. These results could be explained as follows. 5FU was dissolved in CS solution and added to PAsp solution to prepare nanoparticles. When n^+/n^- increased, more CS solution was used. That is to say, more 5FU dissolved in CS solution was added to the PAsp solution resulting in the decrease of

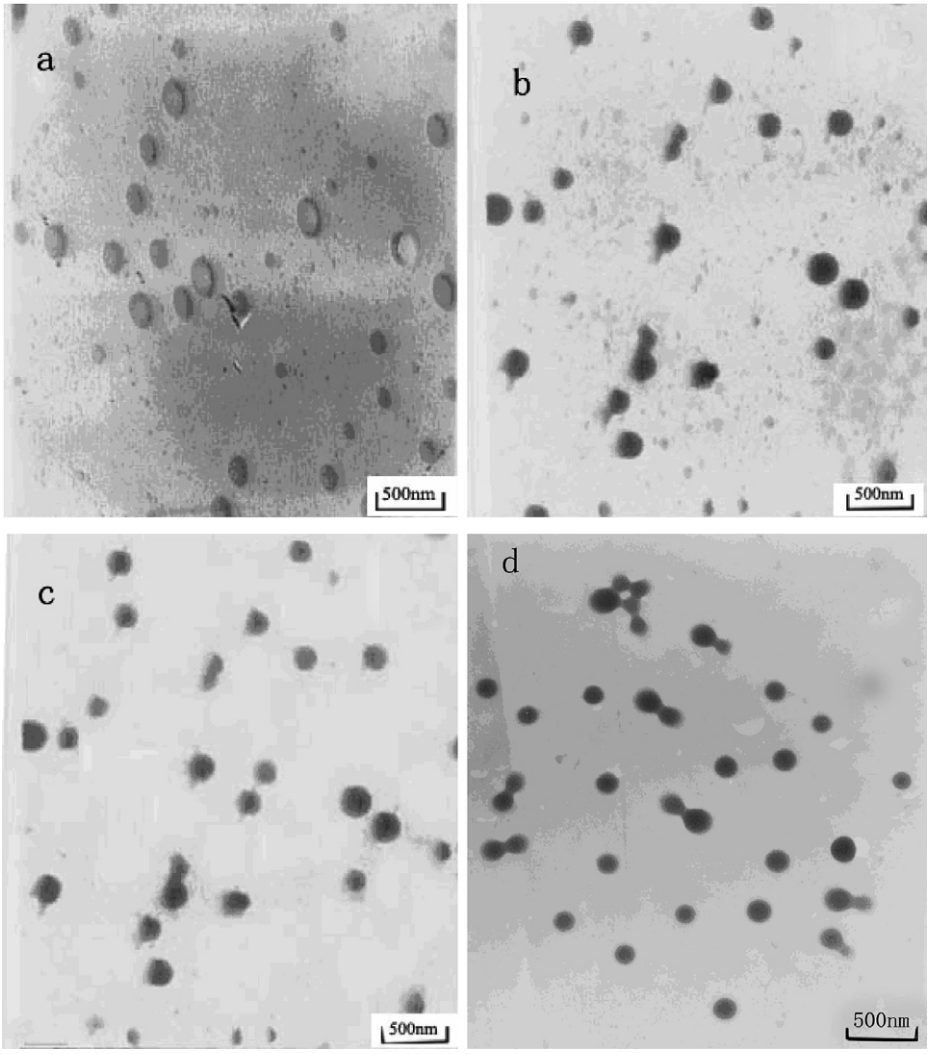

Fig. 4. The TEM images of CS-PAsp-a nanoparticles loading 5FU by absorption with different absorption times. a = 0, b = 0.5 h, c = 2.0 h, and d = 16 h. $n^+/n^- = 2.8$.

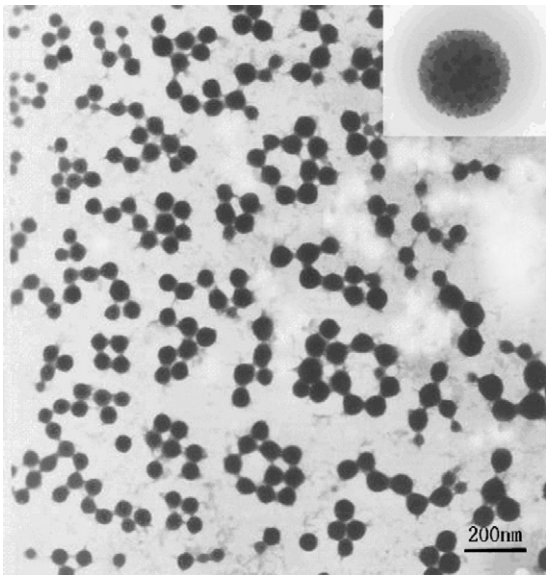

Fig. 5. The TEM image of CS-PAsp-m nanoparticles loading 5FU by mixing method. $n^+/n^- = 1.44$.

EE. Compared to EE, the change of LC was slight. This may result from many factors such as the increase of the nanoparticles weight and EE.

3.3.3. In vitro release

In vitro release of 5FU into PBS solution was evaluated of pure 5FU and CS-PAsp-m nanoparticles with n^+/n^- 1.44 formulated with 5FU LC 37.1% and CS-PAsp-a nanoparticles with n^+/n^- 2.8 formulated with 5FU LC 28.6%.

The release profile is shown in Fig. 6. Pure 5FU escaped rapidly from the dialysis bag 90.1% within the first 0.5 h and the release of 5FU was complete 100% by 7 h. The profiles of the CS-PAsp-a showed a rapid release of 5FU about 95% (w/w) within the first 7 hours, but a slow release of 5FU about 80% in 192 h after being cross-linked (G-CS-PAsp-a). To the nanoparticles CS-PAsp-m, the release profile of 5FU showed much slowly compared to the CS-PAsp-a. As seen in Fig. 6, the nanoparticles without being cross-linked released 5FU gradually up to 96% (w/w) in 96 h after the start of the release test, and slowly to 53% in 192 h after being cross-linked (G-CS-PAsp-m). We thought that in the case of absorption method, most of 5FU molecules associated near the nanoparticles surface diffused out easily and caused the rapid release in the incubation time. However, when mixing method was employed, 5FU embedded into the nanoparticles might be bonded to PAsp by ionic reaction resulting in 5FU diffusion out

Table 10
Encapsulation efficiency (EE) and loading capacity (LC) of CS-PAsp-m nanoparticles loading 5FU by mixing method ($n^+/n^- = 1.44$)

CS:PAsp	0.8	1.44	1.6	3.2
EE (%)	49.9	45.9	40.2	30.1
LC (%)	33.3	37.1	34.9	32.5

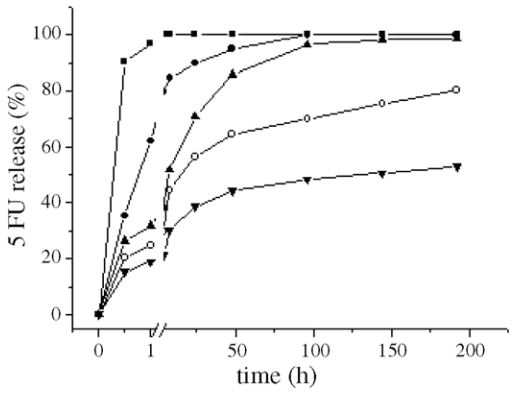

Fig. 6. In vitro release profile of pure 5FU (■), drug-loaded nanoparticles CS-PAsp-a (●, $n^+/n^- = 2.8$), G-CS-PAsp-a (○, $n^+/n^- = 2.8$), CS-PAsp-m (▲, $n^+/n^- = 1.44$), and G-CS-PAsp-m (▼, $n^+/n^- = 1.44$).

slowly. Being cross-linked, 5FU released slowly, and the reason might be due to the formation of denser film on the surface of the nanoparticles.

3.3.4. Pharmacokinetics study

According to the chromatogram, the control plasma did not affect the sample separation and determination. The

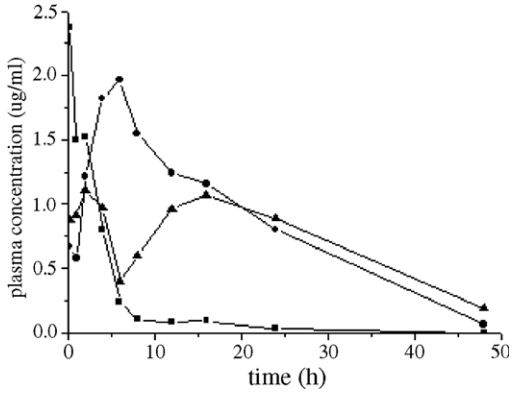

Fig. 7. 5FU plasma concentration in mice after oral administration of 5FU solution (■), drug-loaded nanoparticles G-CS-PAsp-m (●, $n^+/n^- = 1.44$) and G-CS-PAsp-a (▲, $n^+/n^- = 2.8$). Each point represents the mean value of six animals.

Table 9
Mean size and size distribution of CS-PAsp-m nanoparticles before and after loading 5FU by mixing method ($n^+/n^- = 1.44$)

CS:PAsp	0.8		1.44		1.6		3.2	
	Free	Load	Free	Load	Free	Load	Free	Load
D_h (nm)	98.6	152.8	185.8	188.3	184.2	206.0	147.5	220.5
PI	0.14	0.07	0.12	0.14	0.09	0.14	0.13	0.15

Table 11
Pharmacokinetic parameters of 5FU after i.v. administration of 5FU injection and drug-loaded CS-PAsp nanoparticles injection in mice

Pharmacokinetic parameters	5FU	Absorption method	Mixing method
$AUC_{(0-48\ h)}$ (μg h/mL)	8.58	40.46	34.22
$MRT_{(0-48\ h)}$ (h)	5.07	14.74	18.46
$T_{1/2}$ (h)	4.19	7.37	12.36
$K(\lambda z)$ (1/h)	0.1656	0.0941	0.0561
C_{max} (μg/mL)	2.3769	1.9677	1.1031
$AUC_{(0-\infty)}$ (μg h/mL)	8.59	41.14	37.64
$MRT_{(0-\infty)}$ (h)	5.09	15.46	22.76

$T_{1/2}$, half life time; C_{max}, maximal concentration; AUC, area under (the plasma concentration time) curve; $K(\lambda z)$, elimination rate constant; MRT, mean residence time.

average recovery and accuracy of the determination method was greater than 90%. Fig. 7 shows the 5FU plasma concentration – time profile after administration of 5FU solution, G-CS-PAsp-a and G-CS-PAsp-m suspension. To G-CS-PAsp-a, the plasma 5FU concentration raised quickly to the maximum concentration (C_{max}) of 1.1 ng/mL at 2.0 h (t_{max}). After that the plasma 5FU level decreased sharply to 0.4 ng/mL by 6.0 h, then started to rise slowly again, reaching a second maximum plasma level of 1.07 ng/mL on 16 h, followed by a steady decrease to 0.18 ng/mL at 48 h. G-CS-PAsp-m had a different release profile. The plasma 5FU level decreased from 0.67 to 0.58 ng/mL at the first hour after administration and then raised quickly to the maximum concentration (C_{max}) of 1.97 ng/mL at 6.0 h (t_{max}), followed by a slow decrease to 0.07 ng/mL at 48 h. In contrast, the pure 5FU solution had a much higher maximum concentration (C_{max}) of 2.38 ng/mL at 0.25 h and quickly decreased to 0.1 ng/mL at 8.0 h. When the administration extended to 48 h, the 5FU level decreased to zero. In addition, the area under the curve (AUC) was 40.46 μg h/mL for G-CS-PAsp-a and 34.22 μg h/mL for G-CS-PAsp-m, but only 8.58 μg h/mL for 5FU solution (Table 11). The drug-loaded CS-PAsp nanoparticles presented a sustained release of 5FU compared to the 5FU solution, the half-life times were prolonged and the areas under curve (AUC) were increased.

4. Conclusion

The formation of new polyelectrolyte chitosan-PAsp nanoparticles with predetermined nano-metric size and morphological structure can be simply manipulated and controlled by varying the key processing conditions, including chitosan to PAsp unit molar ratio, solution pH, incubation temperature, ionic strength, and cross-linker concentration. After the loading of a model drug 5FU by mixing and absorption method, higher encapsulation was attained, furthermore, the size of CS-PAsp nanoparticles did not considerably increase and narrow size distribution was maintained. In vitro and in vivo experiment of the drug-loaded nanoparticles showed CS-PAsp nanoparticles encapsulation presented a sustained release of 5FU compared to the 5FU solution and the areas under curve (AUC) were increased.

Acknowledgements

This work was supported by National Science Foundation of China (Grant No. 50403011) and STCSM (0452nm065, 05QMX1404, and 05DJ14005).

References

[1] D. Lochmanna, E. Jaukb, A. Zimmer, Drug delivery of oligonucleotides by peptides, Eur. J. Pharm. Biopharm. 58 (2004) 237–251.
[2] W.P. Cheng, A.I. Gray, L. Tetley, T.L.B. Hang, A.G. Schatzlein, I.F. Uchegbu, Polyelectrolyte nanoparticles with high drug loading enhance the oral uptake of hydrophobic compounds, Biomacromolecules 7 (2006) 1509–1520.
[3] C. Peniche-Covas, W. Argüelles-Monal, Sorption and desorption of water vapour by membranes of the polyelectrolyte complex of chitosan and carboxymethyl cellulose, Polym. Int. 38 (1995) 45–52.
[4] I.C. Liao, A.C.A. Wan, E.K.F. Yim, K.W. Leong, Controlled release from fibers of polyelectrolyte complexes, J. Control. Release 104 (2005) 347–358.
[5] S.R. Jameela, A. Jayakrishnan, Glutaraldehyde cross-linked chitosan microspheres as a long acting biodegradable drug delivery vehicle: studies on the in vitro release of mitoxantrone and in vivo degradation of microspheres in rat muscle, Biomaterials 16 (1995) 69–775.
[6] F. Maestrelli, M. Garcia-Fuentes, P. Mura, M.J. Alonso, A new drug nanocarrier consisting of chitosan and hydoxypropyleyclodextrin, Eur. J. Pharm. Biopharm. 63 (2006) 79–86.
[7] C. Schtz, J.M. Lucas, C. Viton, A. Domard, C. Pichot, T. Delair, Formation and properties of positively charged colloids based on polyelectrolyte complexes of biopolymers, Langmuir 20 (2004) 7766–7778.
[8] C. Schatz, A. Domard, C. Viton, C. Pichot, T. Delair, Versatile and efficient formation of colloids of biopolymer-based polyelectrolyte complexes, Biomacromolecules 5 (2004) 1882–1892.
[9] H.Q. Mao, K. Roy, W.L. Troung-Le, K.A. Janes, K.Y. Lin, Y. Wang, J.I. August, K.W. Leong, Chitosan-DNA nanoparticles as gene carriers: synthesis, characterization and transfection efficiency, J. Control. Release 70 (2001) 399–421.
[10] Y.L. Zheng, Y. Wu, W.L. Yang, C.C. Wang, S.K. Fu, X.Z. Shen, Preparation, Characterization, and drug release in vitro of chitosan-glycyrrhetic acid nanoparticles, J. Pharm. Sci. 95 (2006) 179–191.
[11] Y. Boonsongrit, A. Mitrevej, B.W. Mueller, Chitosan drug binding by ionic interaction, Eur. J. Pharm. Biopharm. 62 (2006) 267–274.
[12] K. Kataoka, Design of nanoscopic vehicles for drug targeting based on micellisation of amphiphillic block copolymers, Pure Appl. Chem. A31 (1994) 759–769.
[13] T. Ehtezazi, T. Govender, S. Stolnik, Hydrogen bonding and electrostatic interaction of as cationic drug with polyaspartic acid, Pharm. Res. 17 (2000) 871–878.
[14] P. Guenoun, H.T. Davis, M. Tirrell, J.W. Mays, Aqueous micellar solutions of hydrophobically modified polyelectrolytes, Macromolecules 29 (1996) 3965–3969.

[15] H.L. Jiang, K.J. Zhu, Comparison of poly(aspartic acid) hydrogel and poly(aspartic acid)/gelatin complex for entrapment and pH-sensitive release of protein drugs, J. Appl. Polym. Sci. 9 (2006) 2320–2329.
[16] G.J. Peters, J. Lankelma, R.M. Kok, P. Noordhuis, C.J. Vangroeningen, C.L. Vanderwilt, S. Meyer, H.M. Pinedo, Prolonged retention of high-concentrations of 5-fluorouracil in human and murine tumors as compared with plasma, Cancer Chemother. Pharmacol. 31 (1993) 269–276.
[17] G. Francini, R. Petrioli, A. Aquino, S. Gonnelli, Advanced breast-cancer-treatment with folinic acid, 5-fluorouracil, and mitomycin-c, Cancer Chemother. Pharmacol. 32 (1993) 359–364.
[18] P.M. Calabro-Jones, J.E. Bylield, J.F. Ward, Time–dose relationships for 5-fluorouracil cytotoxicity against human epithelial cancer cells in vitro, Cancer Res. 42 (1982) 4413–4420.
[19] M. Simeonova, R. Velichkova, G. Ivanova, V. Enchev, I. Abrahams, Poly(butylcyanoacrylate) nanoparticles for toptical delivery of 5-fluorouracil, Int. J. Pharm. 263 (2003) 133–140.
[20] E. Elvire Fournier, C. Passirani, N. Colin, P. Breton, S. Sagodira, J.P. Benoit, Development of novel 5FU-loaded poly(methylidene malonate 2.1.2)-based microspheres for the treatment of brain cancers, Eur. J. Pharm. Biopharm. 57 (2004) 189–197.
[21] Y. Wu, W.L. Yang, C.C. Wang, J.H. Hu, S.K. Fu, Chitosan nanoparticles as a novel delivery system for ammonium glycyrrhizinate, Int. J. Pharm. 295 (2005) 235–245.
[22] T. Qurashi, H.S. Blair, S.J. Allen, Studies on modified chitosan membranes. I. Preparation and characterization, J. Appl. Polym. Sci. 46 (1992) 255–261.
[23] T. Nakato, A. Kusuno, T. Kakuchi, Synthesis of poly (succinimide) by bulk polycondensation of L-aspartic acid with an acid catalyst, J. Polym. Sci. Pol. Chem. 38 (2000) 117–122.
[24] B. Chu, Z.L. Wang, J.Q. Yu, Dynamic light scattering study of internal motions of polymer coils in dilute solution, Macromolecules 24 (1991) 6832–6838.
[25] X. Wang, Y. Li, J. Li, J. Wang, Y. Wang, Z. Guo, H. Yan, Salt effect on the complex formation between polyelectrolyte and oppositely charged surfactant in aqueous solution, Phys. Chem. B 109 (2005) 10807–10812.
[26] A. Zintchenko, G. Rother, H. Dautzenberg, Transition highly aggregated complexes-soluble complexes via polyelectrolyte exchange reactions: kinetics, structural changes, and mechanism, Langmuir 19 (2003) 2507–2513.
[27] Y.T. Wu, C. Grant, Effect of chelation chemistry of sodium polyaspartate on the dissolution of calcite, Langmuir 18 (2002) 6813–6820.
[28] C.L. de Vasconcelos, P.M. Bezerril, D.E.S. dos Santos, et al., Effect of molecular weight and ionic strength on the formation of polyelectrolyte complexes based on poly(methacrylic acid) and chitosan, Biomacromolecules 7 (2006) 1245–1252.
[29] Q. Chen, Y. Hu, Y. Chen, X.Q. Jiang, Y.H. Yang, Microstructure formation and property of chitosan-poly (acrylic acid) nanoparticles prepared by macromolecular complex, Macromol. Biosci. 5 (2005) 993–1000.
[30] H. Dautzenberg, Polyelectrolyte complex formation in highly aggregating systems methodicalaspects and general tendencies, in: Physical Chemistry of Polyelectrolytes, T. Radeva (Ed.), Dekker, New York, 2001, p. 743.